

Distributions of Critical Load in Arrays of Nanopillars

Zbigniew Domański and Tomasz Derda

Abstract—Arrays of vertical pillars are encountered in a variety of nanotechnological applications, e.g. in sensing systems. If such an array of N pillars, with pillars characterized by random strength thresholds σ_{th} , is subjected to a sufficiently large axial load F_c , the pillars break in the form of cascades of avalanches. Using a Fiber Bundle Model with a so-called local load transfer rule from destroyed pillars to the intact ones, we analyze distributions of F_c when thresholds σ_{th} are independently drawn from the Weibull distribution, $p_{k,\lambda}(\sigma_{th}) = (k/\lambda)(\sigma_{th}/\lambda)^{k-1} \exp[-(\sigma_{th}/\lambda)^k]$, where $\lambda = 1$ and k are the scale and shape, respectively. Based on simulations we show that distribution of $F_c/N = \sigma_c$ can be well fitted by the Weibull pdf $p_{K,\Lambda}(\sigma_c) = (K/\Lambda)(\sigma_c/\Lambda)^{K-1} \exp[-(\sigma_c/\Lambda)^K]$, where K and Λ are functions of k and N . Specifically, for $N \gg 1$, the mean $\langle F_c/N \rangle \sim \ln(k)$.

Index Terms—avalanche, array of pillars, critical load, fracture, probability distribution.

I. INTRODUCTION

A MODERN nanodevice may be composed of a large number of identical parts that function as a unit. A possible sequence of failures among these components decreases the device performance and may eventually lead to a catastrophic avalanche of failures.

Majority of studies dealing with avalanches of failures employ so-called load transfer models, as e.g., the Fibre Bundle Model (FBM) or Random Fuse Model [1], [2], [3]. Especially the FBM, originally designed to describe loaded fibre bundles, can be applied to model damage processes in an array of vertical pillars regularly distributed on a flat substrate.

In this work, the array of pillars is represented by a collection of fibers and then analyzed within a static Fibre Bundle Model framework [4], [5], [6], [7], [8], [9]. Breaking of pillars from the support is a process involving avalanches of fractures. This means that when a pillar breaks, its load is transferred to the other intact elements and thus the probability of subsequent fractures increases. Based on the results of numerical simulations, we claim that the observed weakening of the axial load F_c is related to a load transfer phenomenon which is an inherent part of the fracture process in a bundle of pillars [8]. In our numerical experiment a set of $N = L \times L$ pillars, located in the nodes of the supporting square lattice, is subjected to an axial load F . Defects significantly influence the mechanical behaviour of materials under load. Due to these defects, the pillar-strength-thresholds are modelled by quenched random variables. The two most popular strength-thresholds distributions are uniform distribution and Weibull

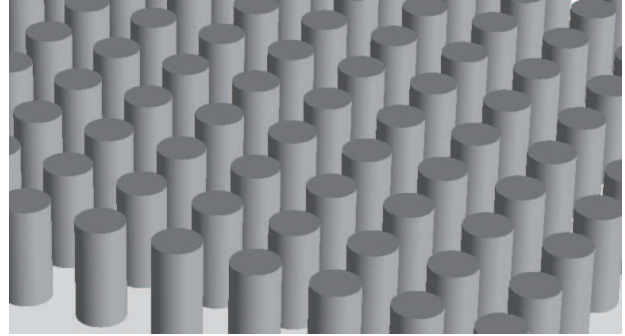


Fig. 1. Schematic view of an array of pillars.

distribution. Strength-thresholds reflect multiple breaking modes related by von Mises type, Coulomb-Mohr or other failure criteria [10], [11]. The mechanism of load transfer is a key aspect of the model and it can be classified into two main groups: global (equal) load sharing (GLS) and local load sharing (LLS). There are also mixtures of these rules and other rules e.g., range variable rule, hierarchical model [12], [13], [14]. In the GLS model, long-range interactions are assumed as all the intact elements equally share a load of a failed element. The GLS rule can be applied if the support-pillar interface is perfectly rigid.

II. MATHEMATICAL MODEL AND COMPUTATION METHOD

In this work, we assume that the support-pillar interface has a certain compliance, thus the load redistribution becomes localized. We employ the LLS transfer mode - within a short interval between consecutive fractures the load carried by the broken pillar is transferred only to its closest intact elements. Because of such a limited-range-load-transfer, the distribution of load is not homogeneous giving rise to appearance of regions of stress accumulation throughout the entire system. The increasing stress on the intact pillars leads to other failures, after which each intact pillar bears growing load. If the load transfer does not trigger further fractures, a stable configuration emerges meaning that this initial value of F is not sufficient to provoke fracture of the entire system, and its value has to be increased by an amount δF . In the simulations we applied a quasi-static loading procedure - if the system is in a stable state the external load is uniformly increased on all the intact pillars just to destroy only the weakest intact pillar.

A series of increases in the value of the external load gives F_c which induces an avalanche of failures among all still undestroyed pillars. Application of quasi-static loading allows one to obtain minimal load F_c necessary for destruction of all the pillars in the system. In order to compare results for different system sizes, critical loads F_c are scaled by the appropriate initial system sizes $\sigma_c = F_c/N$.

Manuscript received April 7, 2017.

Z. Domański is with the Institute of Mathematics, Czestochowa University of Technology, Dabrowskiego 69, PL-42201 Czestochowa, Poland. (corresponding author e-mail: zbigniew.domanski@im.pcz.pl).

T. Derda is with the Institute of Mathematics, Czestochowa University of Technology, Dabrowskiego 69, PL-42201 Czestochowa, Poland. (e-mail: tomasz.derda@im.pcz.pl).

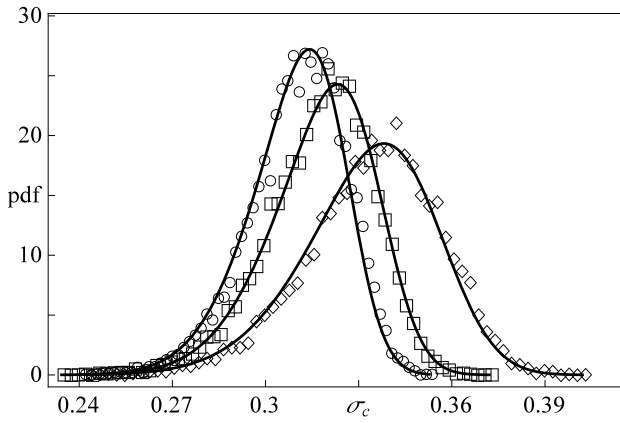


Fig. 2. Empirical probability density functions (pdf) of σ_c for arrays with $L = 100$ (circles), $L = 70$ (squares) and $L = 40$ (diamonds). Weibull index $k = 2$ for all presented pdfs. The solid lines represent skew-normally distributed σ_c with the parameters computed from the simulations.

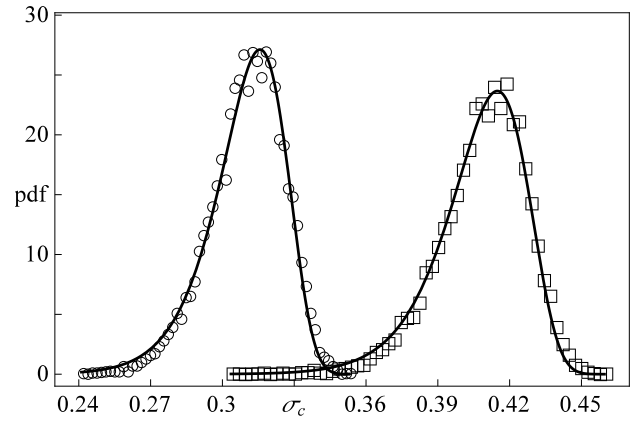


Fig. 3. Empirical probability density functions (pdf) of σ_c for arrays with $L = 100$: $k = 2$ (circles) and $k = 4$ (squares). The solid lines represent Weibull distributed σ_c with the parameters computed from the simulations.

In this paper, pillar-strength-thresholds σ_{th} are drawn from the Weibull distribution [15], [16]. The probability density function of this distribution is given by

$$p_{k,\lambda}(\sigma_{th}) = (k/\lambda)(\sigma_{th}/\lambda)^{k-1} \exp[-(\sigma_{th}/\lambda)^k] \quad (1)$$

Parameters $k > 0$ and $\lambda > 0$ define the shape and scale of this pdf. Shape parameter k (also called Weibull index) controls the amount of disorder in the system. Without loss of generality, we assume $\lambda = 1$ and thus the corresponding probability density reads

$$p_{k,1}(\sigma_{th}) = k\sigma_{th}^{k-1} \exp[-\sigma_{th}^k] \quad (2)$$

We address a question how these local critical loads distributed according to (2) combine to create an effective-global critical load F_c . Based on our numerical simulations, we have found that coefficient of skewness of the F_c distribution is a decreasing function of the system size which takes negative values for systems with $L > 10$. For this reason we employ two distributions for fitting our skewed data, namely:

- (i) three-parameter skew normal distribution (SND) [17], [18] defined by

$$p(\sigma_c) = \frac{\exp[-\frac{(\sigma_c - \xi)^2}{2\omega^2}] \operatorname{erfc}[-\frac{\alpha(\sigma_c - \xi)}{\sqrt{2}\omega}]}{\sqrt{2\pi}\omega} \quad (3)$$

where ξ , ω , α are location, scale and shape parameters, respectively.

- (ii) the Weibull distribution:

$$p_{K,\Lambda}(\sigma_c) = (K/\Lambda)(\sigma_c/\Lambda)^{K-1} \exp[-(\sigma_c/\Lambda)^K] \quad (4)$$

It is worth mentioning that for the GLS rule, σ_c obeys normal distribution for both Weibull and uniform distribution of pillar-strength thresholds.

III. RESULTS AND DISCUSSION

Based on the Fibre Bundle Model and local load sharing rule, we developed a program code for the simulation of the loading process in two-dimensional nanopillar arrays. Intensive numerical simulations are conducted for systems ranging from $N = 5 \times 5$ to $N = 100 \times 100$. We have tuned the amount of pillar-strength-threshold disorder by integer

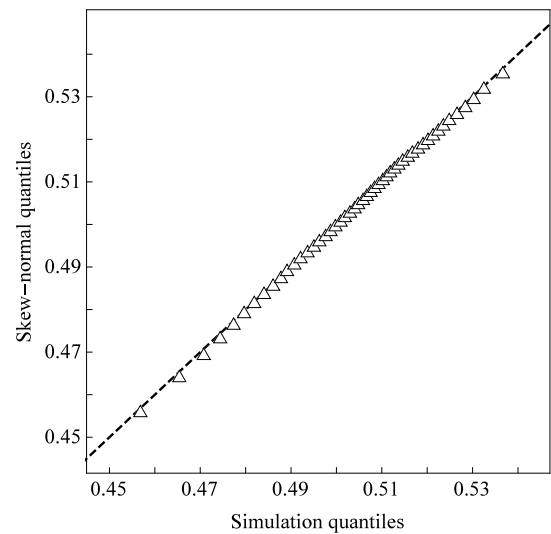


Fig. 4. The Q-Q plot of the quantiles of the set of computed σ_c vs the quantiles of the skew normal distribution. System size $N = 100 \times 100$ and $k = 7$.

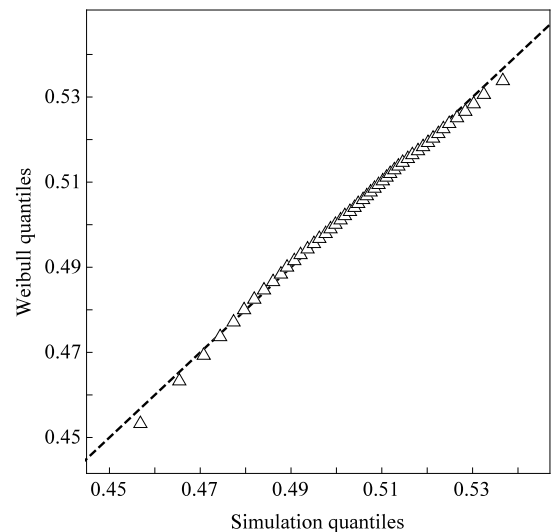


Fig. 5. The Q-Q plot of the quantiles of the set of computed σ_c vs the quantiles of the Weibull distribution. System size $N = 100 \times 100$ and $k = 7$.

values of k ranging from 2 to 9. In order to get reliable statistics, each simulation was repeated 10^4 times.

Figures 2 and 3 show empirical probability density functions of σ_c for chosen systems. In these plots we have also added fitting lines of skew normal (Fig. 2) and Weibull (Fig. 3) probability density functions with parameters computed from the samples. It can be seen that both of these theoretical distributions are in good agreement with empirical distributions of σ_c . We also present a quantile-quantile plot (Q-Q plot) of the quantiles of the collected data set against the corresponding quantiles given by the SND and Weibull probability distributions. From Figures 4 and 5, it is seen that the result of fitting by skew normal distribution is slightly better than the Weibull fitting. Based on simulations, we have observed that fitting by skew normal distribution gives better results than Weibull fitting for all analysed systems, especially for the smaller ones. However, it should be noted that skew normal distribution has one parameter more than Weibull distribution. Fitting by Weibull distribution allows us to analyse the influence of system properties on the microscopic level (Weibull distributed pillar-strength thresholds) on the macroscopic response (distribution of critical loads) in the framework of one type of distribution. Hence, we focus our attention on the fitting of σ_c distribution by Weibull distribution.

In the case of Weibull distribution, values of the fitted parameters K and Λ depend on system size and Weibull index k in the original distribution characterizing the pillar's strength. The plots of the parameters K and Λ are shown in Figures 6 and 7, respectively. For a fixed value of k , the parameter K is a strictly increasing function of linear system size L . We have found that this relation can be approximated by the following formula

$$K_k(L) = a_1 + a_2\sqrt{L} + a_3 \ln L \quad (5)$$

Weibull index	Fitted parameter		
	a_1	a_2	a_3
$k = 2$	-2.505	0.019	5.916
$k = 4$	-0.293	-0.315	6.813
$k = 6$	0.534	-0.584	7.880
$k = 9$	2.320	-0.550	8.264

where a_1, a_2, a_3 are fitted parameters. One can also see that fitted curves are (increasingly) ordered according to Weibull index k .

Contrary to K , the parameter Λ is a strictly decreasing function of L , which can be fitted by the formula (see Fig. 7)

$$\Lambda_k(L) = b_1 + \frac{b_2}{\sqrt{L}} \quad (6)$$

Weibull index	Fitted parameter	
	b_1	b_2
$k = 2$	0.270	0.454
$k = 4$	0.371	0.463
$k = 6$	0.441	0.473
$k = 9$	0.515	0.468

where b_1, b_2 are matched parameters. The ordering of curves, reported for the previous plot, is preserved.

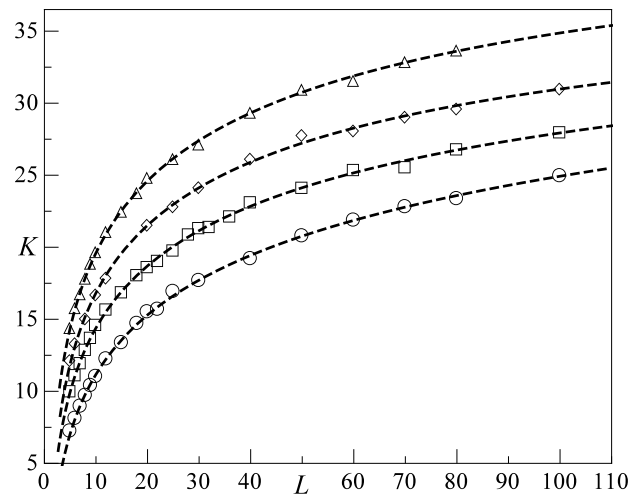


Fig. 6. Parameter K as a function of L , formula (5), for different values of Weibull index: $k = 2$ (circles), $k = 4$ (squares), $k = 6$ (diamonds), $k = 9$ (triangles).

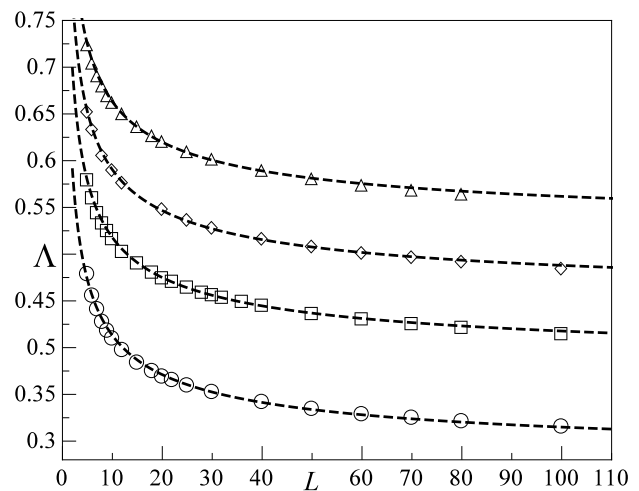


Fig. 7. Parameter Λ as a function of L , formula (6), for different values of Weibull index: $k = 2$ (circles), $k = 4$ (squares), $k = 6$ (diamonds), $k = 9$ (triangles).

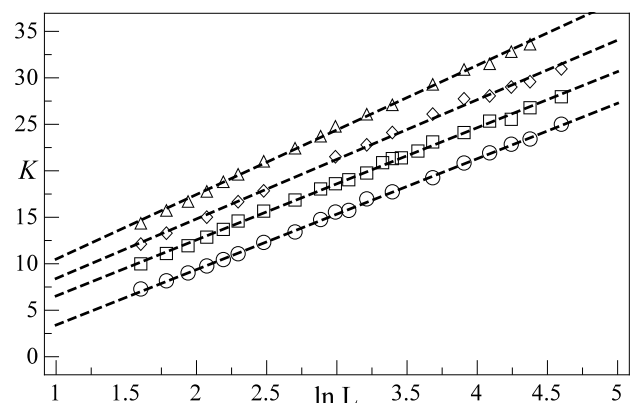


Fig. 8. Same as in Fig. 6, parameter K vs $\ln L$ for different values of Weibull index: $k = 2$ (circles), $k = 4$ (squares), $k = 6$ (diamonds), $k = 9$ (triangles). The dashed lines represent a linear function with fitted parameters.

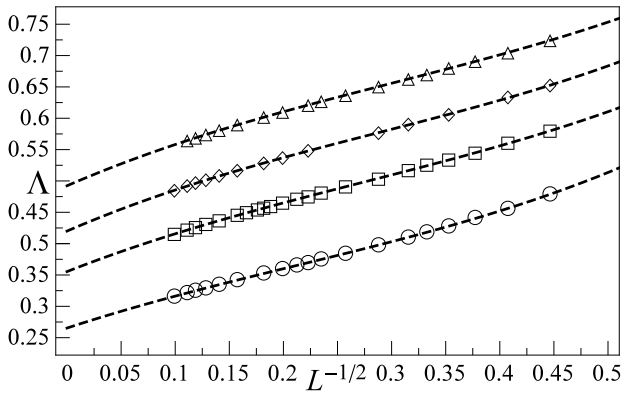


Fig. 9. Same as in Fig. 7, parameter Λ vs $1/\sqrt{L}$ for different values of Weibull index: $k = 2$ (circles), $k = 4$ (squares), $k = 6$ (diamonds), $k = 9$ (triangles). The dashed lines represent third degree polynomial with fitted parameters.

One of the components of the formula (5) is the natural logarithm of L . If the linear system size is logarithmized, the parameter K can be approximated by the linear function - it is reported in Fig. 8. In turn, Fig. 9 presents values of the parameter Λ in the function of $L^{-1/2}$ which is a part of the function 6. In this case we applied a third degree polynomial as an approximative formula.

Taking assumption that F_c/N follows Weibull distribution with the parameters K and Λ , the expected value of this distribution is given by

$$E[F_c/N] = \langle F_c/N \rangle = \Lambda \Gamma(1 + \frac{1}{K}) \quad (7)$$

where $\Gamma(1 + \frac{1}{K})$ is the gamma function. From the fitting we have obtained $K \in (7.27, 33.69)$. Substituting limits of this interval into the relation

$$\Gamma(1 + \frac{1}{K}) / \Gamma(1) \quad (8)$$

we received two values 0.94 and 0.98. As it was previously mentioned, K is a increasing function of the system size, therefore relation (8) tends to unity with the increasing system size. Consequently, the parameter Λ is a key factor of the formula (7) and the mean critical load can be roughly estimated by

$$\langle F_c/N \rangle \sim \Lambda \Gamma(1) = \Lambda \quad (9)$$

In the following we propose a universal formula for calculating Λ in dependence of L and k . The function (6) can be rewritten as

$$\Lambda(L, k) = b_1(k) + \frac{b_2(k)}{\sqrt{L}} \quad (10)$$

where parameters b_1, b_2 are replaced by their functions of k . The plot of the parameters b_1 and b_2 with values obtained from simulations is shown in Fig. 10. We have approximated $b_1(k)$ and $b_2(k)$ by

$$b_1(k) = c_1 + c_2 \ln k \quad (11)$$

with $c_1 \approx 0.148$, $c_2 \approx 0.165$ and

$$b_2(k) = d_1 + d_2 k \quad (12)$$

with $d_1 \approx 0.451$, $d_2 \approx 0.002$. It can be noticed that $b_2(k)/\sqrt{L} \rightarrow 0$ when $L \rightarrow \infty$ and so Λ depends only on $b_1(k)$.

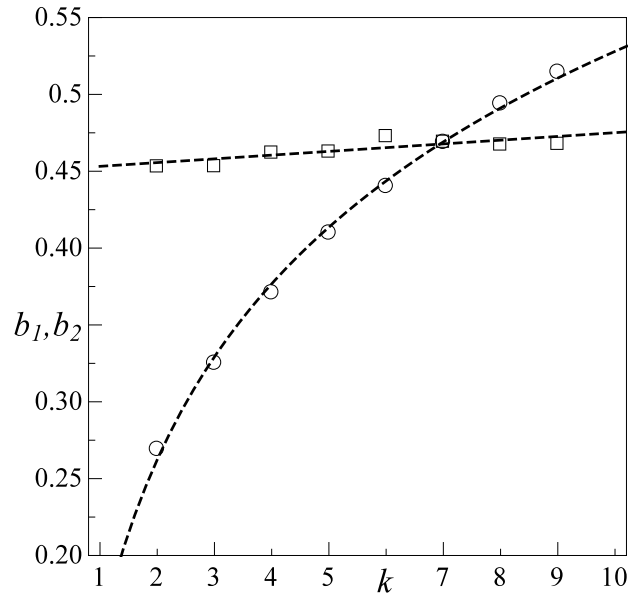


Fig. 10. Parameters b_1 (circles) and b_2 (squares) vs index k . The dashed lines illustrate functions (11) and (12) with fitted parameters.

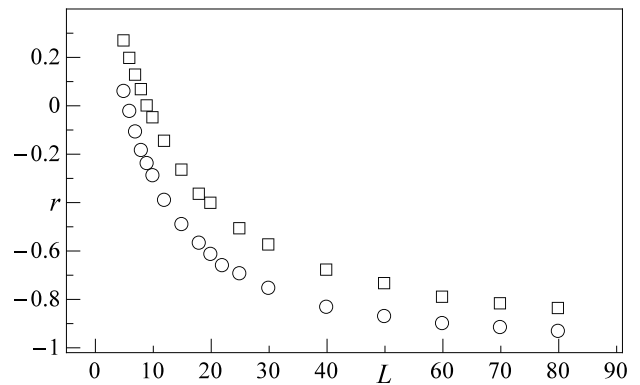


Fig. 11. The Pearson correlation coefficient r between two variables F_c and Δ_c versus the linear system size. Circles represent results for the systems with $k = 2$, whereas squares represent systems with $k = 9$.

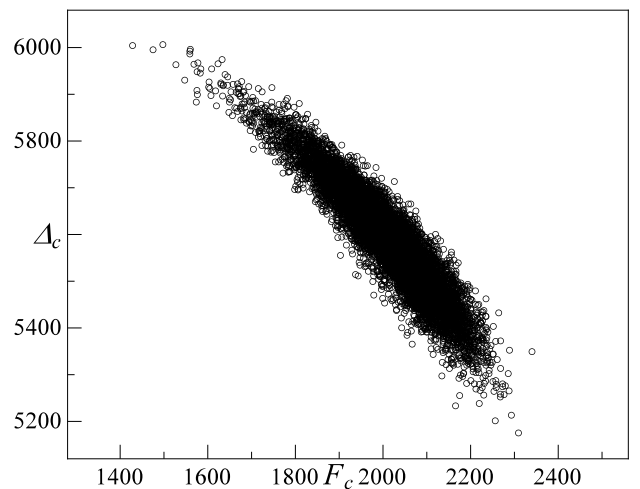


Fig. 12. Size of critical avalanche Δ_c vs critical load F_c for arrays of $N = 80 \times 80$ pillars taken from 10^4 samples.

Some insight into the strength of the system can be gained by collating, sample by sample, the critical force F_c with the number Δ_c of pillars crushed under this force, i.e., since the load increases in a quasi-static way then $\Delta_c + 1$ pillars bear safely the load $F_c - \delta F$ which means that the average maximal stress $\bar{\sigma}_{\max}$ supported by the system has an upper bound

$$\bar{\sigma}_{\max} < \frac{F_c}{\Delta_c} \quad (13)$$

We employ Pearson correlation coefficient r to measure the relationship between critical loads F_c and sizes of critical avalanches Δ_c . The results of r as a function of L are illustrated in Fig. 11. For the smallest systems we obtained positive values of the coefficient r , but as the system size is increased the values of r decrease and become negative. In the smallest systems there is no relationship between F_c and Δ_c whilst systems with $L > 40$ are characterised by a strong negative relationship for all analysed k . For the clarity of the plot shown in Fig. 11 we report only the results for two values of k . An exemplary scatter plot of Δ_c versus F_c is shown in Fig. 12.

In conclusion, we have studied numerically effective distributions of critical loads F_c in quasi-statically loaded arrays of nanopillars. By fitting discrete distributions of critical loads, we have found how the random pillar-strength-thresholds influence the macroscopic yield of the system. Valuable results of this work involve two observations: (i) if the pillar-strength-thresholds obey the Weibull distribution, the critical load is also distributed according to the Weibull pdf and (ii) the corresponding parameters K and Λ , i.e., global scale and shape parameters, are functions of k , where the parameter k characterizes the local property of the system.

REFERENCES

- [1] C. Manzato, A. Shekhawat, P. K. V. V. Nukala, M. J. Alava, J. P. Sethna, and S. Zapperi, "Fracture Strength of Disorder Media: Universality, Interactions, and Tail Asymptotics," *Phys. Rev. Lett.*, vol. 108, id. 065504, Feb. 2012.
- [2] Z. Bertalan, A. Shekhawat, J.P. Sethna, and S. Zapperi, "Fracture strength: Stress concentration, extreme value statistics and the fate of the Weibull distribution," *Phys. Rev. Applied*, vol. 2, id. 034008, Sept. 2014.
- [3] S. Zapperi, P. Ray, H.E. Stanley, and A. Vespignani, "Analysis of damage clusters in fracture processes," *Phys. A*, vol. 270, pp. 57-62, 1999.
- [4] D. Sornette, "Elasticity and failure of a set of elements loaded in parallel," *J. of Physics A: Mathematical and General*, vol. 22, No. 6, pp. L243-L251, 1989.
- [5] A. Hansen, P.C. Hemmer, and S. Pradhan, "The Fiber Bundle Model: Modeling Failure in Materials," Wiley, 2015.
- [6] S. Pradhan, A. Hansen A., and B.K. Chakrabarti, "Failure processes in elastic fiber bundles," *Rev. Mod. Phys.*, vol. 82, pp. 499-555, 2010.
- [7] M.J. Alava, P.K.V.V. Nukala, and S. Zapperi, "Statistical models of fracture," *Adv. In Physics*, vol. 55, pp. 349-476, 2006.
- [8] F. Kun, F. Raischel, R.C. Hidalgo, and H.J. Herrmann, "Extensions of fibre bundle models," *Modelling Critical and Catastrophic Phenomena in Geoscience, Lecture Notes in Physics*, vol. 705, pp. 57-92, 2006.
- [9] Z. Domański, T. Derda, and N. Sczygiol, "Critical avalanches in fiber bundle models of arrays of nanopillars," in *Lecture Notes in Engineering and Computer Science: Proceedings of The International MultiConference of Engineers and Computer Scientists 2013, IMECS 2013*, 13-15 March, 2013, Hong Kong, pp. 765-768.
- [10] F. Raischel, F. Kun, and H.J. Herrmann, "A simple beam model for the shear failure of interfaces," *Phys. Rev. E*, vol. 72, id. 046126, Oct. 2005.
- [11] J. Knudsen and A.R. Massih, "Breakdown of disordered media by surface loads," *Phys. Rev. E*, vol. 72, id. 036129, Sept. 2005.
- [12] R.C. Hidalgo, Y. Moreno, F. Kun, and H.J. Herrmann, "Fracture model with variable range of interaction," *Phys. Rev. E*, vol. 65, id. 046148, 2002.
- [13] R.C. Hidalgo, S. Zapperi, and H.J. Herrmann, "Discrete fracture model with anisotropic load sharing," *J. Stat. Mech.*, id. P01004, 2008.
- [14] T. Derda, "Analysis of damage processes in nanopillar arrays with hierarchical load transfer," *J. Appl. Math. Comput. Mech.*, vol. 15(3), pp. 27-36, 2016.
- [15] W. Weibull, "A statistical distribution function of wide applicability," *J. Appl. Mech.*, vol. 18, pp. 293-297, 1951.
- [16] N.M. Pugno and R.S. Ruoff, "Nanoscale Weibull statistics," *J. Appl. Phys.*, vol. 99, id. 024301, 2006.
- [17] A. Azzalini and A.R. Massih, "A class of distributions which includes the normal ones," *Scand. J. Statist.*, vol. 12, pp. 171-178, 1985.
- [18] A. Azzalini, "The Skew-Normal and Related Families," Cambridge University Press, 2013.